

# Separated-Transport-Recombination p-i-n Photodiode for High-Speed and High-Power Performance

Jin-Wei Shi, H.-C. Hsu, F.-H. Huang, W.-S. Liu, J.-I. Chyi, Ja-Yu Lu, C.-K. Sun, and Ci-Ling Pan

**Abstract**—We demonstrate a novel p-i-n photodiode (PD) structure, the separated-transport-recombination PD, which can greatly relieve the tradeoffs among the resistance-capacitance bandwidth limitation, responsivity, and output saturation power performance. Incorporating a short carrier lifetime (less than 1 ps) epitaxial layer to serve as a recombination center, this device exhibits superior speed and power performance to a control PD that has a pure intrinsic photoabsorption layer. Our demonstrated structure can also eliminate the bandwidth degradation problem of the high-speed photodetector, whose active photoabsorption layer is fully composed of short lifetime ( $\sim 1$  ps) materials, under high dc bias voltages.

**Index Terms**—Photodiode (PD), high-power photodiode, optical receivers.

RECENTLY, the development of the optical amplifier has created a new demand for high-speed photodiodes (PDs) with high saturation power performance. Some novel receiver circuits use fiber amplifiers as preamplifiers, thus relieving or even eliminating the necessity of wide-bandwidth electrical amplifiers [1], [2]. However, ultrahigh-speed PDs are known to suffer from the problem of bandwidth degradation under intense optical power illumination [1]–[3]. There are several ways to provide photodetectors with wide electrical bandwidth and enable them to achieve high output saturation power performance [1], [2], such as, the velocity matched distributed photodetector [4], evanescently coupled PD [5], [6], partially depleted absorber PDs [7], low-temperature-grown GaAs (LTG-GaAs)-based photodetectors [8], and untravelling carrier PDs [1], [2], [9], [10]. Among those reported techniques, downscaling the depletion layer thickness is the most straightforward way to increase the saturation power of a PD [1], [7]. However, PDs with thin depletion layers usually suffer from the problems of low quantum efficiency and very limited resistance-capacitance ( $RC$ ) bandwidth. In this letter, we demonstrate a novel p-i-n PD structure: the separated-transport-recombination PD (STR-PD), which can greatly relieve the tradeoffs among output saturation power, quantum efficiency, and electrical bandwidth performance. For our demonstrated GaAs-based STR-PD, we adopted the LTG-GaAs layer, which has an extremely short carrier lifetime

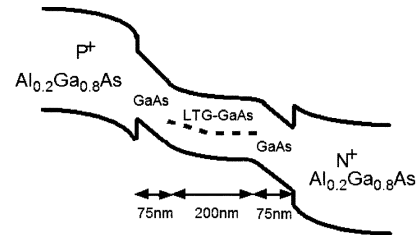


Fig. 1. Conceptual band diagram of the demonstrated STR-PD.

(less than 1 ps) [11], to serve as the recombination center in the active photoabsorption region. Compared with the control p-i-n PD with a pure intrinsic GaAs-based photoabsorption layer, the demonstrated device exhibits superior electrical bandwidth performance under a higher output current regime without seriously sacrificing responsivity, especially under low dc bias voltages ( $-1$  V).

Fig. 1 shows a conceptual band diagram of the STR-PD. The LTG-GaAs layer with an extremely short carrier lifetime [11] serves as a recombination center sandwiched between two high-quality GaAs-based photoabsorption layers. As shown in Fig. 1, the external applied electric field is concentrated in the two GaAs layers due to the high defect density and field-screening effect of the inserted LTG-GaAs layer [12]. These two photoabsorption layers can, thus, be treated as a “transport layer” or “depletion layer” in our structure due to their much higher mobility compared to LTG-GaAs and the concentration of the applied electric field. To recombine the photogenerated carriers, which exhibit low drift velocity under high current operation [1], the position of this inserted LTG-GaAs based layer is located near the center of the photoabsorption region [1]. Under optical illumination, most of the photogenerated electrons in the transport layer, which is near the  $P^+$   $Al_{0.2}Ga_{0.8}As$  layer, will be injected into the LTG-GaAs layer and will recombine with the photogenerated hole from the other side of transport layer. However, some injected and photogenerated carriers in the edge of the LTG-GaAs layer, where the electric field is much stronger and the drift distance is much shorter than in the other part of the recombination layer [8], can still escape from defects and can contribute to the measured photocurrent. In the case of our demonstrated device, by assuming a 0.2-ps carrier lifetime of the LTG-GaAs layer and a maximum saturation velocity ( $\sim 1 \times 10^5$  m/s) of the carriers near the edge of recombination layer, we can get a calculated value of the escape probability of around 10% [8]. We can, thus, conclude that most of the injected carriers from the transport layers (around 90%) will be recombined by defects, and that the effective carrier-drift distance in the STR-PD will be roughly approximated by the thickness of the one-sided GaAs-based photoabsorption (depletion) layer, which can be thinned down to shorten the drift time of

Manuscript received December 12, 2004; revised February 25, 2005. This work was supported by National Science Council of Taiwan under Grant NSC 92-2218-E-008-011- and Grant 93-2215-E-008-022-.

J.-W. Shi, H.-C. Hsu, F.-H. Huang, W.-S. Liu, and J.-I. Chyi are with the Department of Electrical Engineering, National Central University, Taoyuan 320, Taiwan, R.O.C. (e-mail: jwshi@ee.ncu.edu.tw).

J.-Y. Lu and C.-K. Sun are with the Graduate Institute of Electro-Optical Engineering, National Taiwan University, Taipei 106, Taiwan, R.O.C.

C.-L. Pan is with the Institute of Electro-Optical Engineering, National Chaio Tung University, Hsinchu, 300, Taiwan, R.O.C.

Digital Object Identifier 10.1109/LPT.2005.850886

TABLE I  
EPI-LAYER STRUCTURE OF THE DEMONSTRATED STR-PD. DEVICES A AND B HAVE SIMILAR EPI-LAYER STRUCTURES EXCEPT FOR THE PHOTOABSORPTION REGION

	Material	Thickness (nm)		
N contact layer	N <sup>+</sup> -GaAs	10nm		
Cladding layer	N <sup>+</sup> -Al <sub>0.2</sub> Ga <sub>0.8</sub> As	400nm		
Graded bandgap layer	N <sup>+</sup> -Graded layer	20nm		
Photo-absorption region	Device A	Device B	Device A	Device B
	GaAs	GaAs	75nm	350nm
	LTG-GaAs		200nm	
	GaAs		75nm	
Graded bandgap layer	P <sup>+</sup> -Graded layer	20nm		
Cladding layer	P <sup>+</sup> -Al <sub>0.2</sub> Ga <sub>0.8</sub> As	400nm		
Optical isolation layers	Al <sub>0.5</sub> Ga <sub>0.5</sub> As	2000nm		
Buffer layer	GaAs	200nm		
Substrate	S.I. GaAs	100 $\mu$ m		

photogenerated carriers and increase the output saturation current. In our structure, the tradeoff between the output saturation current and  $RC$  bandwidth limitation can also be relieved significantly due to the increase in the thickness of the total intrinsic ( $i$ ) layer, which is composed of undoped GaAs and LTG-GaAs layers with high resistivity, and to the reduction of the device capacitance without affecting the carrier drift time. Compared with the traditional p-i-n PD, it can minimize the  $RC$  bandwidth limitation by increasing the thickness of the intrinsic photoabsorption layer directly. However, the drift time will be increased and the output saturation power will be seriously degraded [1]. Regarding the traditional LTG-GaAs-based p-i-n PD [13], its entire photoabsorption region is composed of LTG-GaAs, and the external applied electric field in this layer is weak due to the field-screening effect of the LTG-GaAs based PD under reverse bias voltages [12]. The weak electric field will result in a significant reduction of the drift velocity of photogenerated carriers and the quantum efficiency performance. On the other hand, the high electric field in the LTG-GaAs-based photoabsorption layer will cause the breakdown problem and lifetime increasing effect [8], [14]–[16], which will seriously degrade the speed of the device. Due to the separation of the transport layer (GaAs) from the recombination layer (LTG-GaAs) in our STR-PD structure, the applied electric field will be concentrated in the two GaAs-based transport layers, and the problems of low drift velocity and lifetime increasing effect of the LTG-GaAs based layer can, thus, be compromised.

In order to study the influence of the recombination layers on the high-power performance of PDs, two kinds of devices, which have the same epilayer structure except for the photoabsorption active region, were fabricated. As shown in Fig. 1, device A has an LTG-GaAs-based recombination layer with a 200-nm thickness in the center of the photoabsorption region, and the thickness of the surrounding GaAs layer is 75 nm. Device B has a pure GaAs-based photoabsorption layer with a 350-nm thickness, which is around five times thicker than the effective carrier-drift distance of device A (350 versus 75 nm). Table I provides details about the epilayer structure of these two devices. The two types of fabricated devices have the same geometry of the traveling-wave PD [13], which can achieve band-

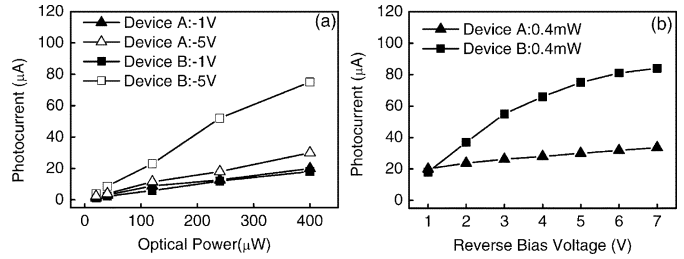


Fig. 2. (a) Measured photocurrent versus the optical pumping power of devices A and B under different reverse bias voltages ( $-1$  and  $-5$  V), and (b) the measured photocurrent versus the dc reverse bias voltages of devices A and B under a fixed optical pumping power (0.4 mW). Triangle: Device A. Square: Device B. The active areas of devices A and B are both  $400 \mu\text{m}^2$ .

width-efficiency product performance superior to that of vertical-illuminated PDs [1].

We employed a mode-locked Ti:sapphire laser, which has a center wavelength of 850 nm, as the light source for dc photocurrent and ac transient measurements. Fig. 2(a) and (b) shows the input optical power and dc bias voltage versus the measured photocurrent of both devices with the same device-absorption-length ( $200 \mu\text{m}$ ) and active area ( $400 \mu\text{m}^2$ ), respectively. Even under the highest reverse bias voltage ( $-7$  V), the measured dark current of both devices was just around  $\sim 200$  nA. This value was much smaller than the measured photocurrent and has been excluded from the data points shown in Fig. 2. In Fig. 2(a), we can clearly see that the responsivity of device A under a  $-5$ -V dc bias voltage is nearly one half of that of device B ( $\sim 0.19$  A/W versus  $\sim 0.08$  A/W) due to the recombination center inserted in its active photoabsorption region. However, under a low bias voltage ( $-1$  V), the responsivity of device B degraded seriously and was close to that of device A ( $0.05$  A/W). The significant decrease in responsivity of device B under a low dc bias voltage ( $-1$  V) indicates that it suffers from a serious space-charge screening effect [1]–[3] and saturation of its output current. Increasing the applied dc bias voltage of the PD can minimize the space-charge screening effect under high optical power illumination. As for device A, it has a much shorter carrier-drift distance (75 versus 350 nm) and a stronger electric field located in the GaAs-based photoabsorption layer than does device B. We can, thus, expect that device A will have a much lower external dc bias voltage to saturate the velocity of the photogenerated holes and overcome the space-charge screening effect than will device B. The traces of the bias dependent photocurrent under a fixed optical power excitation, shown in Fig. 2(b), clearly reveal different degrees of the space-charge screening effect in both devices. Compared with device A, device B exhibits a much more significant increase of photocurrent with the increasing dc bias voltage under high optical power excitation (0.4 mW) due to that higher dc bias voltage is necessary to minimize the space-charge screening effect and recover the value of responsivity in the case of device B with a relatively thick depletion layer.

We performed an ac transient measurement in both devices with similar geometric sizes ( $400 \mu\text{m}^2$ ). The 3-dB bandwidth of the measurement system was about 10 GHz, which corresponds to nearly 40-ps time resolution. Fig. 3(a) and (b) shows the full-width at half-maximum (FWHM) of the measured impulse responses versus average optical pumping power and reverse bias voltage, respectively. As the diagrams indicate,

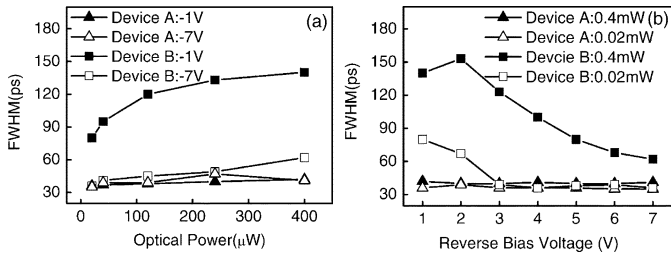


Fig. 3. (a) FWHM of the measured impulse responses of both devices under different levels of optical pumping power with fixed dc reverse bias voltages ( $-1$  and  $-7$  V), and (b) under different dc reverse bias voltages with fixed levels of optical pumping power (0.02 and 0.4 mW). Triangle: Device A. Square: Device B. The active areas of devices A and B are both  $400 \mu\text{m}^2$ .

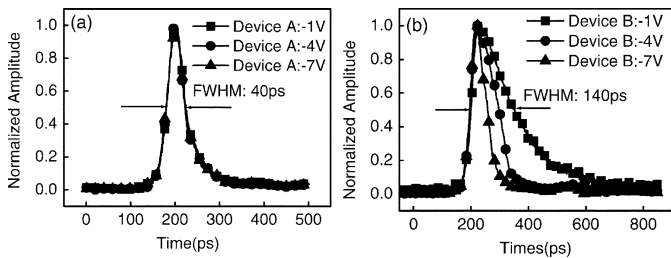


Fig. 4. Normalized impulse responses of (a) device A and (b) device B with a  $400\text{-}\mu\text{m}^2$  active area under a fixed optical pumping power (0.4 mW) and different reverse bias voltages ( $-1$ ,  $-4$ ,  $-7$  V).

device A achieved better speed performance than device B, especially under a high output photocurrent and low dc bias voltage. Furthermore, we can clearly see that in the case of device A, the measured FWHM was insensitive to both the reverse bias voltages ( $-1 \sim -7$  V) and input optical power (0.02, 0.4 mW). The traditional LTG-GaAs-based p-i-n or metal-semiconductor-metal PDs, whose photoabsorption regions are fully composed of LTG-GaAs, usually suffer from significant bandwidth degradation under a high external applied electric field ( $> 4.4 \times 10^4$  V/cm) [15], [16] due to the coulomb-barrier lowering and lifetime increasing effects [14]–[16]. As shown in Fig. 3(b), the lifetime increasing effect of the traditional LTG-GaAs-based p-i-n PD under a high dc bias voltage [14]–[16] is eliminated in our novel structure due to the concentration of the applied electric field in the GaAs based transport layers. Fig. 4(a) and (b) shows the normalized impulse responses of devices A and B under a fixed optical excitation power (0.4 mW) and different reverse bias voltages, respectively. We can clearly see that the traces of device A do not exhibit a significant long-tail phenomenon and broaden significantly even under high power excitation (0.4 mW) and a high bias voltage ( $-7$  V). The measured FWHM shown in Fig. 4(a) with 0.4-mW injected optical power was around 40 ps, and the corresponding Fourier-transformed bandwidth was 10 GHz, which was close to the system-limited bandwidth ( $\sim 10$  GHz). On the other hand, the normalized impulse responses of device B, as shown in Fig. 4(b), show serious broadening and the long-tail phenomenon under the same optical excitation power (0.4 mW) and reverse bias voltage ( $-1$  V) as in device A. Even with a high reverse bias voltage ( $-7$  V), device B still exhibits poorer speed performance and a larger FWHM of the measured impulse responses ( $\sim 62$  versus  $\sim 40$  ps) compared to device A under a much lower dc bias voltage ( $-1$  V).

In conclusion, we have demonstrated a novel epilayer structure for a PD, the STR-PD. By inserting a material with a short carrier lifetime that serves as the recombination center in the active photoabsorption region, we can improve the output saturation current and reduce the RC bandwidth limitation significantly without seriously affecting the responsivity performance, especially under a low dc reverse bias voltage ( $-1$  V). The optoelectronic measurement results for the demonstrated device are very promising.

## REFERENCES

- [1] K. Kato, "Ultrawide-band/high-frequency photodetectors," *IEEE Trans. Microw. Theory Tech.*, vol. 47, no. 7, pp. 1265–1281, Jul. 1999.
- [2] H. Ito, S. Kodama, Y. Muramoto, T. Furuta, T. Nagatsuma, and T. Ishibashi, "High-speed and high-output InP-InGaAs untravelling-carrier photodiodes," *IEEE J. Sel. Topics Quantum Electron.*, vol. 10, no. 4, pp. 709–727, Jul/Aug. 2004.
- [3] Y.-L. Huang and C.-K. Sun, "Nonlinear saturation behaviors of high-speed p-i-n photodetectors," *J. Lightw. Technol.*, vol. 18, no. 2, pp. 203–212, Feb. 2000.
- [4] L. Y. Lin, M. C. Wu, T. Itoh, T. A. Vang, R. E. Muller, D. L. Sivco, and A. Y. Cho, "High-power high-speed photodetectors design, analysis, and experiment demonstration," *IEEE Trans. Microw. Theory Tech.*, vol. 45, no. 8, pp. 1320–1331, Aug. 1997.
- [5] F. Xia, J. K. Thomson, M. R. Gokhale, P. V. Studenkov, J. Wei, W. Lin, and S. R. Forrest, "A asymmetric twin-waveguide high-bandwidth photodiode using a lateral taper coupler," *IEEE Photon. Technol. Lett.*, vol. 13, no. 8, pp. 845–847, Aug. 2001.
- [6] S. Demiguel, N. Li, X. Li, X. Zheng, J. Kim, J. C. Campbell, H. Lu, and A. Anselm, "Very high-responsivity evanescently coupled photodiodes integrating a short planar multimode waveguide for high-speed applications," *IEEE Photon. Technol. Lett.*, vol. 15, no. 12, pp. 1761–1763, Dec. 2003.
- [7] X. Li, N. Li, S. Demiguel, X. Zheng, J. C. Campbell, H. H. Tan, and C. Jagadish, "A partially depleted absorber photodiode with graded doping injection regions," *IEEE Photon. Technol. Lett.*, vol. 16, no. 10, pp. 2326–2328, Oct. 2004.
- [8] J.-W. Shi, K. G. Gan, Y.-H. Chen, C.-K. Sun, Y. J. Chiu, and J. E. Bowers, "Ultra-high power-bandwidth product and nonlinear photo-conductance performances of low-temperature-grown GaAs based metal-semiconductor-metal traveling-wave photodetectors," *IEEE Photon. Technol. Lett.*, vol. 14, no. 11, pp. 1587–1589, Nov. 2002.
- [9] T. P. Pearsall, M. Piskorski, A. Brochet, and J. Chevrier, "A  $\text{Ga}_{0.47}\text{In}_{0.53}\text{As}/\text{InP}$  heterophotodiode with reduced dark current," *IEEE J. Quantum Electron.*, vol. QE-17, no. 2, pp. 255–259, Feb. 1981.
- [10] T. Ishibashi, N. Shimizu, S. Kodama, H. Ito, T. Nagatsuma, and T. Furuta, "Uni-traveling-carrier photodiodes," in *Tech. Dig. Ultrafast Electronics Optoelectronics OSA Spring Topical Meeting*, 1997, pp. 166–168.
- [11] S. Gupta, J. F. Whitaker, and G. A. Mourou, "Ultrafast carrier dynamics in III-V semiconductors grown by molecular-beam epitaxy at very low substrate temperatures," *IEEE J. Quantum Electron.*, vol. 28, no. 10, pp. 2464–2472, Oct. 1992.
- [12] J. P. Ibbetson, "Electrical characterization of nonstoichiometric GaAs grown at low temperature by molecular beam epitaxy," Ph.D. Thesis, Univ. of California at Santa Barbara, 1997.
- [13] Y. J. Chiu, S. B. Fleischer, and J. E. Bowers, "High-speed low-temperature-grown GaAs p-i-n traveling-wave photodetector," *IEEE Photon. Technol. Lett.*, vol. 10, no. 7, pp. 1012–1014, Jul. 1998.
- [14] J.-W. Shi, Y.-H. Chen, K. G. Gan, Y. J. Chiu, J. E. Bowers, M.-C. Tien, T.-M. Liu, and C.-K. Sun, "Nonlinear behaviors of low-temperature-grown GaAs-based photodetectors around 1.3- $\mu\text{m}$  telecommunication wavelength," *IEEE Photon. Technol. Lett.*, vol. 16, no. 1, pp. 242–244, Jan. 2004.
- [15] N. Zamdmer, Q. Hu, K. A. McIntosh, and S. Verghese, "Increase in response time of low-temperature-grown GaAs photoconductive switches at high voltage bias," *Appl. Phys. Lett.*, vol. 75, pp. 2313–2315, Oct. 1999.
- [16] J.-W. Shi, Y. J. Chiu, J. E. Bowers, Y.-H. Chen, S.-P. Tai, and C.-K. Sun, "Bias dependent nonlinear responses of LTG-GaAs based p-i-n/n-i-n traveling-wave photodetectors under long wavelength excitation," in *Conf. Lasers and Electro-Optics (CLEO/QELS 2001)*, OSA Tech. Dig., 2001, pp. 20–21.